Convex Relaxation and Decomposition in Large Resistive Power Networks with Energy Storage

Xin Lou and Chee Wei Tan
City University of Hong Kong, Hong Kong

***Abstract*—A fundamental challenge of a smart grid is: to what extent can moving energy through space and time be optimized to benefit the power network with large-scale storage integration? In this paper, we study a dynamic optimal power flow problem with energy storage dynamics in resistive power networks. We first propose a second order cone programming convex relaxation to solve this nonconvex problem optimally. Then, we apply optimization decomposition techniques to decompose and decouple the problem and obtain the global optimal solution in a distributed manner. The optimization decomposition offers new interesting insight over space and time between the dual solution and energy storage dynamics. We investigate the efficiency of the SOCP relaxation in several IEEE benchmark systems and verify that the distributed algorithms can converge fast to the global optimal solution by numerical simulations.**

I. INTRODUCTION

The integration of power flow control, renewable energy and demand response makes the design of communication and control schemes in a smart grid very challenging. Renewable energy is intermittent and difficult to predict and harness, which makes the power flow in the grid hard to control. One efficient way to deal with this is to incorporate energy storage in the grid [1]. Besides, as power price is dynamically changing, energy storage at demand buses can absorb transients while balancing loads. In particular, when the power price is low, users at the demand side can store power in batteries. When the power price is high, e.g., during peak hours, users can consume the energy stored locally at batteries first before consuming the power from the grid. This leads to a well-balanced power flow load and lower power consumption cost.

The Optimal Power Flow (OPF) problem optimizes a network-wide objective, e.g., generation cost or transmission loss, subject to constraints on the power flow, demand requirements and network connectivity. Due to the nonconvexity, OPF is generally hard to solve. In the vast literature on OPF, approximation methodologies, e.g., linearization to obtained the so-called Direct Current (DC) OPF problem by assuming constant voltage and small phase angle has been widely studied [2], [3]. Recently, the authors in [4], [5] demonstrated an interesting zero duality gap result in the OPF problem under mild conditions, and showed that the OPF can be solved exactly or relaxed by Semidefinite Programming (SDP) [6]. For example, the SDP relaxation can be shown to be exact on distribution networks with tree-like network topology [7]. Subsequently, along this line, distributed algorithms have been proposed to solve the resistive network OPF and the general OPF in [8] and [9], respectively.

A fundamental challenge of a smart grid is: to what extent can moving energy through space and time be optimized to benefit the power network with large-scale storage integration? For example, an application is the joint optimization of the power network and electric vehicle charging networks. This dynamic OPF with energy storage are more complex time-dependent power flow optimization problems. In [10], the OPF with energy storage was studied as a linearized OPF problem using the traditional small-angle approximation, and solved using finite horizon optimal control problem for a simple network (a single generator and a single load). Gayme et al [11] formulated a dynamic OPF problem with energy storage and applied the SDP relaxation in [5] to this new setting, but this approach cannot in general guarantee when the SDP relaxation is tight. As a first step towards tackling the challenges in dynamic OPF, we study a dynamic OPF problem in a resistive power network with energy storage dynamics (no phase angle, reactive power variables and reactance parameters). This can be practical in microgrid clusters with renewable energy, e.g., solar power, integration that produces real power flow.

In this paper, we will explore alternate but simpler characterization to global optimality, e.g., Second Order Cone Programming (SOCP) relaxation instead of SDP relaxation for resistive power networks, and also using decomposition methodology [12] that can offer new architectural transformation insight and enable scalable and distributed power flow computation. Overall, the contributions of the paper are as follows:

1) We formulate a dynamic OPF problem with energy storage for resistive power networks, and propose a tight SOCP relaxation for this nonconvex problem.
2) Leveraging the zero duality gap property, we simplify this dynamic OPF by indirect optimization decomposition, which leads to efficient and distributed algorithms that converge fast to the global optimal solution. We also give physical interpretation to the connection between the dual solution in the power flow and energy storage as dynamic marginal price and storage price respectively that give rise to load curve smoothing.
3) Numerical experiments demonstrate the computational efficiency of our SOCP relaxation over SDP relaxation for different IEEE benchmark power systems. Our proposed distributed algorithms also demonstrate fast convergence property.

The work in this paper was partially supported by grants from the Research Grants Council of Hong Kong, Project No. RGC CityU 122013.

II. System Models and Problem Formulations

Let us consider the resistive power network with buses $\mathcal{N} = \{1, 2, \ldots, N\}$ and $\mathcal{E} \subseteq \mathcal{N} \times \mathcal{N}$ transmission lines. In this paper, $\mathcal{G}$ and $\mathcal{D}$ are respectively used to represent the set of generation buses and demand buses. Each bus is attached with an energy storage, i.e., a battery. A bus $i \in \mathcal{D}$ represents the aggregate of users. For each bus i, we denote its one-hop connected neighbors by the set Ω_i and $|\Omega_i| \geq 1$. Furthermore, $\mathbf{Y}$ is the system admittance matrix and we assume that line admittance is symmetric, i.e., $Y_{ij} = Y_{ji} \in \mathbb{R}_{++}$, if $(i,j) \in \mathcal{E}$; $Y_{ij} = Y_{ji} = 0$, otherwise. We use $\mathbf{V}(t)$ and $\mathbf{I}(t)$ to represent the voltage vector $(V_i(t))_{i\in\mathcal{N}}$ and current vector $(I_i(t))_{i\in\mathcal{N}}$ at $t = 1, \ldots, T$, respectively. By Kirchhoff's Current Law and Ohm's Law, we have $\mathbf{I}(t) = \mathbf{Y}\mathbf{V}(t)$. Then, the nodal power and voltage constraints are represented as:

$$\mathbf{V}(t)^\top \mathbf{Y}_i \mathbf{V}(t) \leq \overline{p}_i(t) - r_i(t) \ \ \forall t = 1, \ldots, T, \tag{1}$$

$$\underline{\mathbf{V}} \leq \mathbf{V}(t) \leq \overline{\mathbf{V}} \ \ \forall t = 1, \ldots, T, \tag{2}$$

where $(\cdot)^\top$ denotes transpose, $\mathbf{Y}_i = \frac{1}{2}(\mathbf{E}_i\mathbf{Y} + \mathbf{Y}\mathbf{E}_i)$, $\mathbf{E}_i = \mathbf{e}_i\mathbf{e}_i^\top \in \mathbb{R}^{n\times n}$, $\mathbf{e}_i$ is the standard basis vector in $\mathbb{R}^n$ and $r_i(t)$ is the charge rate (positive) or discharge rate (negative) of bus i at time t. For a generation bus $i \in \mathcal{G}$, $\bar{p}_i(t) > 0$ is the generator capacity. While for a demand bus $i \in \mathcal{D}$, $\bar{p}_i(t) < 0$ and the amount $|\bar{p}_i(t)|$ denotes the minimum power that has to be provided at time t. Similar to [8], we adopt the demand over-satisfaction assumption, i.e., a demand bus can absorb the power $|\bar{p}_i(t)|$ together with additional power to satisfy the basic demand requirement and charge the attached battery.

In addition to the basic OPF constraints, each battery at bus $i \in \mathcal{N}$ has to satisfy:

$$b_i(t+1) \leq b_i(t) + r_i(t) \ \ \forall t = 1, \ldots, T, \tag{3}$$

where (3) takes into account the fact that charge loss or storage leakage can happen in a general battery model. The initial condition of the battery at $i \in \mathcal{N}$ is given by:

$$b_i(1) = B_i^0, \tag{4}$$

where B_i^0 is a positive constant. At each $i \in \mathcal{N}$, $b_i(t)$ and $r_i(t)$ are constrained by:

$$0 \leq b_i(t) \leq B_i \ \ \forall t = 1, \ldots, T+1, \tag{5}$$

$$\underline{r_i} \leq r_i(t) \leq \bar{r_i} \ \ \forall t = 1, \ldots, T, \tag{6}$$

where B_i is the battery capacity at bus i. Finally, let us define two kinds of sets $\mathbb{V}$ and $\mathbb{B}$, which respectively correspond to variables on $\mathbf{V}(t)$ and $\{\mathbf{b}(t), \mathbf{r}(t)\}$, where $\mathbf{b}(t)$ and $\mathbf{r}(t)$ represent $(b_i(t))_{i\in\mathcal{N}}$ and $(r_i(t))_{i\in\mathcal{N}}$, respectively:

$$\mathbb{V} := \{\mathbf{V}(t) | \mathbf{V}(t) \text{ satisfies } (1), (2)\},$$

$$\mathbb{B} := \{(\mathbf{b}(t), \mathbf{r}(t)) | (\mathbf{b}(t), \mathbf{r}(t)) \text{ satisfies } (3) - (6)\}.$$

We are interested in minimizing the transmission loss and the battery cost $h_i(t) = \alpha_i(B_i - b_i(t)) \ \forall i \in \mathcal{N}, t = 1, \ldots, T+1$, i.e., the penalty is proportional to the deviation from the capacity [10]. This is formulated as the following dynamic OPF problem:

$$\begin{aligned} &\text{minimize} \sum_{t=1}^{T} \mathbf{V}(t)^\top \mathbf{Y}\mathbf{V}(t) + \sum_{i\in\mathcal{N}} \sum_{t=1}^{T+1} h_i(t) \\ &\text{subject to } \mathbf{V}(t) \in \mathbb{V}, (\mathbf{b}(t), \mathbf{r}(t)) \in \mathbb{B}, \\ &\text{variables: } \mathbf{V}(t), \mathbf{b}(t), \mathbf{r}(t). \end{aligned} \tag{7}$$

III. Convex relaxation and decomposition

The problem formulation in (7) is a nonconvex Quadratic Constrained Quadratic Programming (QCQP) problem, which is generally hard to solve. In the following, we first introduce an SOCP convex relaxation of (7), show that it is tight, and then propose distributed algorithms to solve it by optimization decomposition techniques.

A. SOCP convex relaxation

We now show that the problem in (7) can be reformulated as an SOCP problem, which is in general computationally more efficient to solve than an SDP relaxation problem obtained in [4], [5]. Introduce the auxiliary variables $X_i(t) = V_i^2(t)$ and $W_{ij}(t) = V_i(t)V_j(t) \ \forall i \in \mathcal{N}, \forall (i,j) \in \mathcal{E}, \ t = 1, \ldots, T$. Let us denote $\mathbf{X}(t)$ and $\mathbf{W}(t)$ by $(X_i(t))_{i\in\mathcal{N}}$ and $(W_{ij}(t))_{(i,j)\in\mathcal{E}}$, respectively. Then, we can rewrite (7) to be equivalent to:

$$\begin{aligned} &\text{minimize} \sum_{i\in\mathcal{N}} \left(\sum_{t=1}^{T} \sum_{j\in\Omega_i} Y_{ij}(X_i(t) - W_{ij}(t)) + \sum_{t=1}^{T+1} h_i(t) \right) \\ &\text{subject to } \sum_{j\in\Omega_i} Y_{ij}(X_i(t) - W_{ij}(t)) \leq \overline{p}_i(t) - r_i(t) \ \forall t = 1, \ldots, T, \\ &\qquad X_i(t)X_j(t) = W_{ij}^2(t) \ \forall (i,j) \in \mathcal{E}, \forall t = 1, \ldots, T, \\ &\qquad \underline{V}_i^2 \leq X_i(t) \leq \overline{V}_i^2 \ \forall i \in \mathcal{N}, \forall t = 1, \ldots, T, \\ &\qquad (\mathbf{b}(t), \mathbf{r}(t)) \in \mathbb{B}, \\ &\text{variables: } \mathbf{X}(t), \mathbf{W}(t), \mathbf{b}(t), \mathbf{r}(t). \end{aligned} \tag{8}$$

Observe that the source of nonconvexity in (8) is the $|\mathcal{E}|T$ constraints: $X_i(t)X_j(t) = W_{ij}^2(t)$. We now relax them to the following inequality constraints:

$$X_i(t)X_j(t) \geq W_{ij}^2(t) \ \forall (i,j) \in \mathcal{E}, \forall t = 1, \ldots, T, \tag{9}$$

which can be rewritten as the equivalent SOCP constraints:

$$\left\| \begin{matrix} 2W_{ij}(t) \\ X_i(t) - X_j(t) \end{matrix} \right\|_2 \leq X_i(t) + X_j(t) \ \forall (i,j) \in \mathcal{E}, \forall t = 1, \ldots, T. \tag{10}$$

Next, we present the following result on the tightness of this SOCP relaxation.

Theorem 1: Solving the SOCP relaxation of (8) with the constraint (10) yields the optimal solution to (7).

Proof: We make the following remarks: 1) The objective function has to be monotonically increasing in $\mathbf{X}(t)$ and decreasing in $\mathbf{W}(t)$ in order to prove that the SOCP relaxation is tight. 2) Variables corresponding to the energy storage part (i.e., $\mathbb{B}$) are linear in (7) and do not appear in the SOCP constraints (10).

To prove the tightness of the SOCP relaxation, we need to show that the constraint in (9) is tight at optimality. Let us first assume that $\mathbf{X}^*(t)$ and $\mathbf{W}^*(t)$ are optimal in the SOCP relaxation. We also assume that there exists a line connecting

bus n_1 and n_2 such that $X^*_{n_1}(t)X^*_{n_2}(t) > W^{*2}_{n_1n_2}(t)$ at t. Also, let us consider a real number $\epsilon_1(t) > 0$ such that $\tilde{X}_{n_i}(t) = X^*_{n_i}(t) - \epsilon_1(t)(i = 1 \text{ or } 2)$. Then, since the objective function is monotonically increasing in $\mathbf{X}(t)$, the optimal value can be made smaller if we replace $X^*_{n_i}(t)$ by $\tilde{X}_{n_i}(t)(i = 1 \text{ or } 2)$. Moreover, if $X^*_{n_1}(t)$ and $X^*_{n_2}(t)$ both hit the lower bounds, we can find a $\epsilon_2(t) > 0$ such that $X^*_{n_1}(t)X^*_{n_2}(t) = \tilde{W}^2_{n_1n_2}(t) = W^{*2}_{n_1n_2}(t) + \epsilon_2(t)$. Since the objective function is decreasing in $\mathbf{W}(t)$, the optimal value can be made smaller if we replace $W^{*2}_{n_1n_2}(t)$ by $\tilde{W}^2_{n_1n_2}(t)$.

To check feasibility, we see that if $X^*_{n_1}(t)$ and $X^*_{n_2}(t)$ both hit the lower bounds, then the nodal power constraints corresponding to line (n_1, n_2) are still feasible when increasing $W^{*2}_{n_1n_2}(t)$ due to the load over-satisfaction assumption. All other constraints are not affected, and thus the problem is still feasible. Similarly, if either $X^*_{n_1}(t)$ or $X^*_{n_2}(t)$ does not hit the lower bound, the nodal power constraints corresponding to line (n_1, n_2) are also feasible when decreasing $X^*_{n_i}(t)(i = 1 \text{ or } 2)$. Also, the nodal voltage constraint still holds. Therefore, $(\mathbf{X}^*(t), \mathbf{W}^*(t))$ is not optimal, which implies that the SOCP relaxation is tight. ■

Remark 1: The SOCP relaxation is tight regardless of the network topology (mesh or tree networks). As the SOCP relaxation of (8) is convex, its Lagrange duality gap is zero under mild conditions [6], which implies that the Lagrange duality gap of (7) is also zero. Capitalizing on this zero duality gap result, we apply optimization decomposition techniques that lead to distributed algorithms to solve (7).

B. Indirect decomposition

In this section, we study an indirect decomposition technique to decompose the dynamic OPF in (7) into simpler subproblems that reveal the coupling over space and time. Figure 1 illustrates the decomposition framework. In the first level, Lagrange dual decomposition is applied. The dual variable corresponding to (1) plays the role of power flow price to control the decomposed subproblems. In the second level, primal decomposition is applied to the energy storage. The primal variable (i.e., the charge/discharge rate $r_i(t)$) plays the role of resource to control the further decomposed subproblems. In the third and last level, Lagrange dual decomposition is applied to (14). The dual variable corresponding to (3) plays the role of energy storage price to control the third-level subproblems. In the following, we explain each decomposed subproblem at each level in details. We first apply the partial dual decomposition to (7). Then, for the subproblems, they are separable in $t = 1, \ldots, T$ and each of them corresponds to one static OPF at time t:

$$\begin{aligned} &\text{minimize } \mathbf{V}(t)^\top \mathbf{Y}\mathbf{V}(t) + \sum_{i\in\mathcal{N}} \lambda_i(t)(\mathbf{V}(t)^\top \mathbf{Y}_i\mathbf{V}(t)) \\ &\text{subject to } \underline{\mathbf{V}} \le \mathbf{V}(t) \le \overline{\mathbf{V}}, \\ &\text{variables: } \mathbf{V}(t). \end{aligned} \tag{11}$$

Although (11) is nonconvex, but due to the zero duality gap, each decomposed subproblem at each t can be solved with the following algorithm proposed in [8].

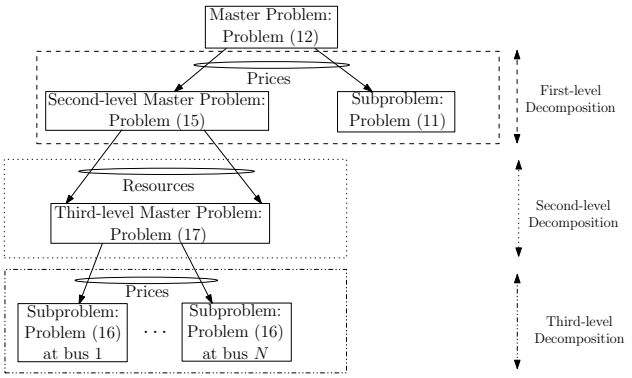

Fig. 1. Indirect optimization decomposition to solve the OPF with energy storage problem in (7). The partial dual decomposition, the primal decomposition and the partial dual decomposition are applied in the respective three levels.

Algorithm 1: Resistive Network Optimal Power Flow

Compute voltage $\mathbf{V}(t)$:

$$V_i^{k+1}(t) = \max\left\{\underline{V}_i, \min\left\{\overline{V}_i, \sum_{j\in\Omega_i} B_{ij}(t)V_j^k(t)\right\}\right\}$$

$\forall i \in \mathcal{N}$, where

$$B_{ij}(t) = \frac{2Y_{ij} + \lambda_i(t)Y_{ij} + \lambda_j(t)Y_{ij}}{2(1+\lambda_i(t))\sum\limits_{j\in\Omega_i} Y_{ij}} \; \forall (i,j) \in \mathcal{E}.$$

Remark 2: Algorithm 1 converges to the unique optimal solution of (11) under mild conditions at each $t = 1, \ldots, T$ [8]. The spectrum of the nonnegative matrix $\mathbf{B}(t)$ in Algorithm 1 captures the solution of (11) analytically in terms of its uniqueness and optimality [8]. It also characterizes the performance of Algorithm 1.

The primary master dual problem is given by

$$\begin{aligned} &\text{maximize} \sum_{t=1}^{T} g(\boldsymbol{\lambda}(t)) + \boldsymbol{\lambda}(t)^\top(\mathbf{r}(t) - \bar{\mathbf{p}}(t)) \\ &\text{subject to } \boldsymbol{\lambda}(t) \ge \mathbf{0} \;\; \forall t = 1, \ldots, T, \\ &\text{variables: } \boldsymbol{\lambda}(t), \end{aligned} \tag{12}$$

where $g(\boldsymbol{\lambda}(t)) = \mathbf{V}^*(t)^\top \mathbf{Y}\mathbf{V}^*(t) + \sum\limits_{i\in\mathcal{N}} \lambda_i(t)(\mathbf{V}^*(t)^\top \mathbf{Y}_i\mathbf{V}^*(t))$.

The dual function is differentiable at each t and it can be solved by the following gradient updates:

$$\lambda_i^{k+1}(t) = [\lambda_i^k(t) + \beta(\mathbf{V}^*(t)^\top \mathbf{Y}_i\mathbf{V}^*(t) - \overline{p}_i(t) + r_i(t))]^+ \; \forall i \in \mathcal{N},$$

where β is the stepsize and $[\cdot]^+$ denotes the projection onto the nonnegative orthant. Next, let us consider the decomposed problem corresponding to the energy storage:

$$\begin{aligned} &\text{minimize} \sum_{t=1}^{T+1} \boldsymbol{\alpha}^\top(\mathbf{B} - \mathbf{b}(t)) + \sum_{t=1}^{T} \boldsymbol{\lambda}(t)^\top \mathbf{r}(t) \\ &\text{subject to } (\mathbf{b}(t), \mathbf{r}(t)) \in \mathbb{B}, \\ &\text{variables: } \mathbf{b}(t), \mathbf{r}(t). \end{aligned} \tag{13}$$

If we apply the primal decomposition to (13), we get the second-level subproblem:

$$\begin{aligned} &\text{minimize } \sum_{t=1}^{T+1} \boldsymbol{\alpha}^\top(\mathbf{B}-\mathbf{b}(t)) + \sum_{t=1}^{T} \boldsymbol{\lambda}(t)^\top \mathbf{r}(t) \\ &\text{subject to } \mathbf{b}(t) \in \mathbb{B}, \\ &\text{variables: } \mathbf{b}(t), \end{aligned} \tag{14}$$

where $\mathbf{r}(t)$ is fixed in $\mathbb{B}$. Note that this second-level subproblem is separable at each $i \in \mathcal{N}$. While for the second-level master problem, we have:

$$\begin{aligned} &\text{minimize } f^*(\mathbf{r}(t)) \\ &\text{subject to } \underline{\mathbf{r}} \le \mathbf{r}(t) \le \bar{\mathbf{r}} \ \ \forall t = 1,\ldots,T, \\ &\text{variables: } \mathbf{r}(t), \end{aligned} \tag{15}$$

where $f^*(\mathbf{r}(t))$ is the optimal value of (13) for given $\mathbf{r}(t)$ $\forall t = 1,\ldots,T$. If we let $\mu_i(t)$ be the dual variable corresponding to (3), then using the subgradient method, we have the following update on the charge/discharge rate at each $t = 1,\ldots,T$:

$$r_i^{k+1}(t) = [r_i^k(t) - \theta(\lambda_i(t) - \mu_i^*(t))]_{\underline{r}_i}^{\overline{r}_i} \ \forall i \in \mathcal{N},$$

where θ is the stepsize and $[\cdot]_y^x$ denotes the projection onto the closed set $[y, x]$ (x and y are the parameters). Furthermore, if we simplify the second-level subproblem (14) by partial dual decomposition, we obtain the third-level subproblems at each $i \in \mathcal{N}$:

$$\begin{aligned} &\text{minimize } \sum_{t=1}^{T+1} \alpha_i(B_i - b_i(t)) + \sum_{t=1}^{T} \mu_i(t)(b_i(t+1) - b_i(t)) \\ &\text{subject to } 0 \le b_i(t) \le B_i, b_i(1) = B_i^0 \ \ \forall t = 1,\ldots,T+1, \\ &\text{variables: } b_i(t). \end{aligned} \tag{16}$$

The third-level master dual problem is given by

$$\begin{aligned} &\text{maximize} \sum_{t=1}^{T} \left(\sum_{i\in\mathcal{N}} g_i(\boldsymbol{\mu}(t)) + (\boldsymbol{\lambda}(t) - \boldsymbol{\mu}(t))^\top \mathbf{r}(t) \right) \\ &\qquad + \boldsymbol{\alpha}^\top(\mathbf{B} - \mathbf{b}^*(T+1)) \\ &\text{subject to } \boldsymbol{\mu}(t) \ge \mathbf{0} \ \ \forall t = 1,\ldots,T, \\ &\text{variables: } \boldsymbol{\mu}(t), \end{aligned} \tag{17}$$

where $g_i(\boldsymbol{\mu}(t)) = \alpha_i(B_i - b_i^*(t)) + \mu_i(t)(b_i^*(t+1) - b_i^*(t))$ in each subproblem of (16). Similarly, the subgradient update of the dual variable $\mu_i(t)$ at each $t = 1,\ldots,T$ is given by:

$$\mu_i^{k+1}(t) = [\mu_i^k(t) - \gamma(b_i^*(t+1) - b_i^*(t) - r_i(t))]^+ \ \forall i \in \mathcal{N},$$

where γ is a stepsize. The above optimization decomposition framework is illustrated in the following algorithm.

Algorithm 2: Jointly Optimal Power Flow and Energy Storage

1) Set the stepsizes $\beta, \theta, \gamma \in (0, 1)$.
2) Calculate the battery amount:

$$b_i^{\ell+1}(t) = \text{argmin}[\sum_{k=1}^{T+1} \alpha_i(B_i - b_i(k)) + \sum_{k=1}^{T} \mu_i^\ell(t)(b_i(k+1) - b_i(k))]_0^{B_i}$$

$\forall i \in \mathcal{N}$ and $\forall t = 1,\ldots,T+1$, subject to $b_i(1) = B_i^0$.

3) Compute:

$$\mu_i^{\ell+1}(t) = [\mu_i^\ell(t) - \gamma(b_i^{\ell+1}(t+1) - b_i^{\ell+1}(t) - r_i^\tau(t))]^+$$

$\forall i \in \mathcal{N}$ and $\forall t = 1,\ldots,T$.
4) Compute:

$$r_i^{\tau+1}(t) = [r_i^\tau(t) - \theta(\lambda_i^l(t) - \mu_i^\ell(t))]_{\underline{r}_i}^{\overline{r}_i}$$

$\forall i \in \mathcal{N}$ and $\forall t = 1,\ldots,T$.
5) Run Algorithm 1 to get $\mathbf{V}^k(t)$, $\forall t = 1,\ldots,T$.
6) Compute:

$$\lambda_i^{l+1}(t) = [\lambda_i^l(t) + \beta(\mathbf{V}^k(t)^\top \mathbf{Y}_i \mathbf{V}^k(t) - \overline{p}_i(t) + r_i^\tau(t))]^+$$

$\forall i \in \mathcal{N}$ and $\forall t = 1,\ldots,T$.
Update β, θ and γ until convergence.

Remark 3: Steps 5 and 6 are equivalent to Algorithm 2 in [8] for fixed $r_i(t)$ at each t, and its convergence proof is given in [8]. Moreover, the subgradient methods of the second-level and third-level master problems (i.e., Steps 3 and 4) can converge to a closed neighborhood of the optimal solution by properly choosing the stepsize [13] and whenever the third-level subgradient updates (i.e., Step 3) runs at a slower timescale than the second-level subgradient updates (i.e., Step 4) and the second-level subgradient updates in turn runs at a slower timescale than the primal gradient updates (i.e., Step 6) [12]. We will show that Algorithm 2 can converge fast to the optimal solution in Section V from different initial points.

Remark 4: Algorithm 2 is carried out in a distributed manner, because each bus only communicates with its local one-hop neighbors (cf. Steps 2, 3 and 4). At Step 5 and 6, each bus exchanges nodal voltage and nodal power price information with its one-hop neighbors.

IV. Energy storage coupling over time interpretation via Lagrange Duality

For the subproblem corresponding to the energy storage, i.e., (13), the Lagrangian at each $i \in \mathcal{N}$ is given by:

$$\begin{aligned} L_i = &\sum_{t=1}^{T+1} \alpha_i(B_i - b_i(t)) + \overline{\mu}_i(t)(b_i(t) - B_i) - \underline{\mu}_i(t) b_i(t) \\ &+ \sum_{t=1}^{T} \lambda_i(t) r_i(t) + \mu_i(t)(b_i(t+1) - b_i(t) - r_i(t)) \\ &+ \overline{\nu}_i(t)(r_i(t) - \overline{r}_i) - \underline{\nu}_i(t)(r_i(t) - \underline{r}_i) + \delta_i(1)(b_i(1) - B_i^0), \end{aligned}$$

where the dual variable $\mu_i(t)$ corresponds to (3), $\underline{\mu}_i(t)$ and $\overline{\mu}_i(t)$ respectively correspond to the lower and upper bound of (5), $\delta_i(1)$ corresponds to (4), and $\underline{\nu}_i(t)$ and $\overline{\nu}_i(t)$ respectively correspond to the discharge and charge bound in (6). As this dynamic OPF has zero duality gap, we use the KKT conditions to deduce the following:

$$\mu_i(t) - \mu_i(t-1) = -\alpha_i + \overline{\mu}_i(t) - \underline{\mu}_i(t) \ \ \forall t = 2, 3, \ldots, T,$$

$$\mu_i(T) = \alpha_i - \overline{\mu}_i(T+1) + \underline{\mu}_i(T+1).$$

TABLE I
COMPARISON OF THE AVERAGE COMPUTATION TIME OF THE SOCP AND THE SDP RELAXATION (IN SECONDS).

Systems	SOCP relaxation	SDP relaxation [4], [5]
14-bus	0.22	0.22
30-bus	0.34	0.56
57-bus	0.51	2.41
118-bus	1.24	14.48
500-bus	3.20	639.91

Interestingly, the difference between two successive dual variables $\mu_i(t)-\mu_i(t-1)$ plays an important role in the decoupling of energy storage dynamics over time: Suppose that battery i never drains or saturates, i.e., $0 < b_i(t) < B_i$, then $\mu_i(t) - \mu_i(t-1) = -\alpha_i$, $\forall t = 2,\ldots,T$ and $\mu_i(T) = \alpha_i$. Thus, $\mu_i(t) = (T-t+1)\alpha_i, \forall t = 1,\ldots,T$. If a battery i drains, then $\mu_i(t) - \mu_i(t-1) \leq -\alpha_i, t = 2,3,\ldots,T$ (drains at t) and $\mu_i(T) \geq \alpha_i$ (drains at $T+1$). If a battery i saturates, then $\mu_i(t) - \mu_i(t-1) \geq -\alpha_i, t = 2,3,\ldots,T$ (saturates at t) and $\mu_i(T) \leq \alpha_i$ (saturates at $T+1$). Therefore, we have the following result:

Lemma 1: For a battery i, if $\mu_i(t-1) - \mu_i(t) < \alpha_i$, where $t = 2,\ldots,T$ or $\mu_i(T) < \alpha_i$, then it is saturated at t or $T+1$; If the inequality is reversed, then battery i is drained at t ($t = 2,\ldots,T$) or $T+1$. If the battery bound of bus i in (7) is inactive $\forall t = 1,\ldots,T$, then $\mu_i(t) = (T-t+1)\alpha_i$.

V. NUMERICAL EXAMPLES AND CASE STUDIES

In this section, we first compare the computational efficiency of our SOCP relaxation with the state-of-the-art SDP relaxation proposed in [4], [5]. Then, we demonstrate a load curve smoothing feature of the dynamic OPF problem in (7) for different energy storage cost. In the last part, we evaluate the performance of our proposed distributed algorithms.

A. Efficiency of SOCP relaxation vs SDP relaxation

We compare the execution time of our SOCP relaxation and the SDP relaxation using interior point algorithms implemented in Matlab, i.e., the CVX software package [14]. The systems used for comparison are the IEEE 14-bus, 30-bus, 57-bus, 118-bus systems, and a 500-bus Polish system during 1999-2000 winter. The data of these IEEE benchmark systems is obtained from [15] and the 500-bus system data is available in MATPOWER [16]. The base power and base voltage are $100MVA$ and $100KV$, respectively. As the data set does not include the storage parameters and time-varying demands, we add feasible problem parameters for the storage and demand in each system for each hour in a day. The experiment is run on a desktop PC with an Intel-i7 CPU and 4G RAM. We solve both the SOCP and SDP relaxation in each system for a hundred times, and record the average computation time to solve (7) in Table I. From Table I, we see that the SOCP relaxation in this OPF problem is much more efficient than the SDP relaxation especially when the network becomes large.

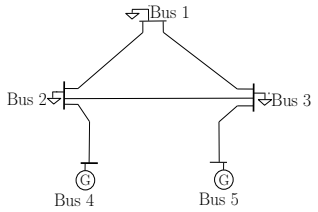

Fig. 2. A 5-bus system ([17], Chapter 6, pp.327). In this system, we assume that each bus has a battery attached to it.

B. Illustration of load curve smoothing in energy storage

We illustrate how energy storage has the benefit of smoothing the load in the network over time using a 5-bus example ([17], Chapter 6, pp.327) in Figure 2. We divide the time period of a day into 6 intervals (every four hours in an interval) and the demand profile starts at 6:00PM, which is a peak hour. After solving this dynamic OPF under the daily demand variation, we can observe a similar load curve smoothing feature like in [18], [19], which we call "valley-filling". Figure 3 is used to illustrate the load curve smoothing feature under different battery cost weights. At the demand valley peak, e.g., 6:00PM, the demand bus discharges the battery and each demand absorbs less power from the grid. Conversely, the battery is charged at the demand valley bottom, e.g., 2:00AM. Thus, the high load usage during peak hours is shifted to valley bottom hours. This feature is prominent when the battery cost is small (cf. Figure 3(a)), i.e., the weight α_i is small. However, when α_i increases, the smoothing effect is limited in order to minimize the total battery cost, and thus smoothing holds only in some intervals, e.g., the load is not balanced at Buses 2 and 3 at some time intervals when we increase α_i to 0.1 as shown in Figure 3(b).

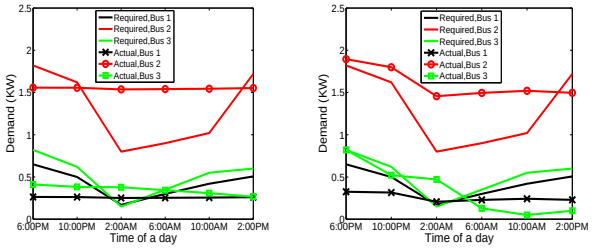

(a) (b)

Fig. 3. Actual and required demand under different α_i $\forall i = 1,2,3$. (a) $\alpha_i = 0.01$ (b) $\alpha_i = 0.1$.

C. Algorithm performance

We evaluate the performance of Algorithm 2 in the 5-bus system using the time-varying demand of a day (6 time intervals) as in Section V-B. The bus topology is illustrated in Figure 2, and a battery is attached each bus. The parameter of the line admittance is $[y_{12}, y_{13}, y_{23}, y_{24}, y_{35}] = [4,3,6,6,7]S$. The initial stepsize are $\beta = 0.3, \theta = 0.02$ and $\gamma = 0.02$. We use the SOCP relaxation as a benchmark to verify the convergence correctness. In Figure 4 and Figure 5, we show

the convergence of Algorithm 2 for 4 buses at 3 time intervals ($t = 1, 3$ and 6) using different initial points. In Figure 4, the initial point is set close to the optimal solution, i.e., in the neighborhood of the optimal solution. We see that it converges very fast to the optimal solution in around 110 iterations. In Figure 5, we see that even when the initial point is set further away from the optimal solution (i.e., we randomly choose a $\boldsymbol{\lambda}^0(t)$), Algorithm 2 also converges fast to the optimal solution, i.e., in less than 210 iterations.

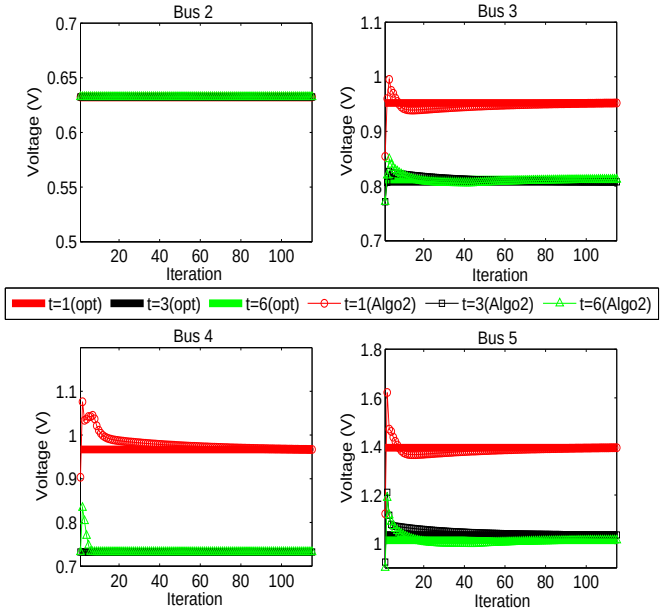

Fig. 4. Illustration of convergence of Algorithm 2 in the 5-bus system with the initial point set close to the optimal solution.

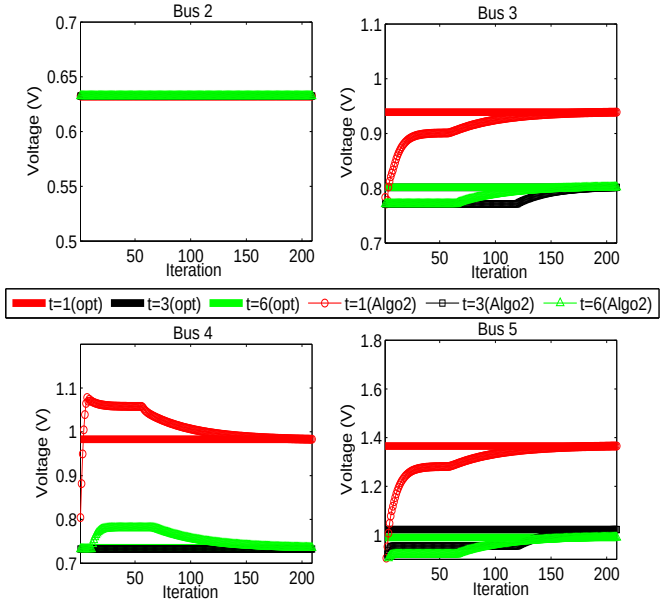

Fig. 5. Illustration of convergence of Algorithm 2 in the 5-bus system with the initial point set further away from the optimal solution.

VI. Conclusion

In this paper, we studied a dynamic OPF problem in resistive power networks with energy storage, which was formulated as a nonconvex QCQP problem. We showed that this nonconvex problem can be solved optimally by an SOCP convex relaxation. We also proposed to decompose the dynamic OPF into simpler subproblems using an indirect optimization decomposition that led to distributed algorithms. The decomposition reveal an interesting coupling over space and time through the Lagrange duality and interpretation of dual solution as prices. We conducted numerical evaluations to show the computational efficiency of the SOCP relaxation over the state-of-the-art SDP relaxation. Finally, we verified that our proposed algorithms could converge fast to the global optimal solution by evaluations under different initial points.

VII. Acknowledgement

The authors acknowledge helpful discussions with Steven H. Low, Desmond W. H. Cai at the California Institute of Technology, and Chin-Woo Tan at Stanford University.

References

[1] J. P. Barton and D. G. Infield. Energy storage and its use with intermittent renewable energy. *IEEE Trans. on Energy Conversion*, 19(2):441–448, 2004.

[2] A. J. Conejo and J. A. Aguado. Multi-area coordinated decentralized DC optimal power flow. *IEEE Trans. on Power Systems*, 13(4):1272–1278, 1998.

[3] H. Wei, H. Sasaki, J. Kubokawa, and J. Yokoyama. An interior point nonlinear programming for optimal power flow problems with a novel data structure. *IEEE Trans. on Power Systems*, 13(3):870–877, 1998.

[4] J. Lavaei, A. Rantzer, and S. H. Low. Power flow optimization using positive quadratic programming. *Proc. of IFAC World Congress*, 2011.

[5] J. Lavaei and S. H. Low. Zero duality gap in optimal power flow problem. *IEEE Trans. on Power Systems*, 27(1):92–107, 2012.

[6] S. Boyd and L. Vanderberghe. *Convex Optimization*. Cambridge University Press, 2004.

[7] J. Lavaei, D. Tse, and B. Zhang. Geometry of power flows and optimization in distribution networks. *Proc. of IEEE PES General Meeting*, 2012.

[8] C. W. Tan, D. W. H. Cai, and X. Lou. DC optimal power flow: uniqueness and algorithms. *Proc. of IEEE SmartGridComm*, 2012.

[9] A. Y. S. Lam, B. Zhang, and D. Tse. Distributed algorithms for optimal power flow problem. *Proc. of IEEE Conf. on Decision and Control (CDC)*, 2012.

[10] M. Chandy, S. H. Low, U. Topcu, and H. Xu. A simple optimal power flow model with energy storage. *Proc. of IEEE Conf. on Decision and Control (CDC)*, 2010.

[11] D. Gayme and U. Topcu. Optimal power flow with distributed energy storage dynamics. *IEEE Trans. on Power Systems*, 28(2):709–717, 2013.

[12] D. P. Palomar and M. Chiang. A tutorial on decomposition methods for network utility maximization. *IEEE Journal on Selected Areas in Communications*, 24(8):1439–1451, 2006.

[13] N. Z. Shor. *Minimization Methods for Non-Differentiable Functions*. Springer-Verlag, Berlin, 1985.

[14] M. Grant and S. Boyd. CVX: Matlab software for disciplined convex programming. *version beta 2.0, http://cvxr.com/cvx*, 2012.

[15] Power System Test Case Archive. University of Washington, Seattle, WA. *Available: http://www.ee.washington.edu/research/*.

[16] R. D. Zimmerman, C. E. Murillo-Sánchez, and R. J. Thomas. MATPOWER's extensible optimal power flow architecture. *Proc. of IEEE PES General Meeting*, 2009.

[17] J. D. Glover, M. S. Sarma, and T. J. Overbye. *Power System Analysis and Design*. Cengage Learning, 5th edition, 2011.

[18] N. Chen, T. Quek, and C. W. Tan. Optimal charging of electric vehicles in smart grid: Characterization and valley-filling algorithms. *Proc. of IEEE SmartGridComm*, 2012.

[19] L. Gan, U. Topcu, and S. H. Low. Optimal decentralized protocol for electric vehicle charging. *IEEE Trans. on Power Systems*, 28(2):940–951, 2013.